# SANGOMA: Stochastic Assimilation for the Next Generation Ocean Model Applications
# EU FP7 SPACE-2011-1 project 283580

Deliverable 5.7:
Result of the data assimilation experiment aiming to estimate Lagrangian sea ice parameters
Due date: 31/10/2015
Delivery date: 31/10/2015
Delivery type: Report, public


Laurent Bertino Alberto Carrassi
NERSC, NORWAY

# Contents

**1 Introduction** **3**

**2 Methodology** **5**

**3 Results** **6**
3.1 Case 1 - Sequential EnKF . . . . . 6
3.2 Case 2 - Asynchronous EnKF (AEnKF) . . . . . 6
3.2.1 Model sensitivity to sea-ice parameters . . . . . 6
3.2.2 AEnKF with sea-ice thickness observations . . . . . 11

**4 Conclusion** **14**

# Chapter 1

# Introduction

The choice of parameter values is crucial in the course of sea ice model developments and for the success of operational Arctic Ocean forecasts and reanalysis products. Similarly to other areas of geoscience, manual tuning of parameters is impractical in sea-ice models as well, making urgent the use Automatic methods for parameter calibration.

The problem of estimating the parameter of a geophysical model is well known in the literature, and it has been treated in the framework of both the Kalman filter-like and variational assimilation (e.g. Jazwinski, 1970; Bennett et al., 1996; Navon, 1997), based on a technique called the state augmentation method (Jazwinski, 1970). Formal conditions for an observing network and data assimilation to provide reliable estimate of the model parameters have been studied in connection with the concept of observability (Cohn and Dee, 1988; Navon, 1997). Successful parameter estimation has been also obtained in the context of simple prototypes of nonlinear dynamics with the EnKF (Anderson, 2001; Aksoy et al., 2006; Yang and Delsole, 2009; Koyama and Watanabe, 2010) and with the maximum likelihood ensemble filter (Zupanski and Zupanski, 2006; Zupanski et al., 2007; Orescanin et al., 2009). Annan and Hargraves (2004) have proposed a method, in the framework of the EnKF, to estimate the parameters of the Lorenz (1963) model and have then successfully applied the same approach to an intermediate complexity Earth system model (Annan et al., 2005). Efficient state and parameter estimation using the EKF has been demonstrated in the context of a coupled ocean-atmosphere model used for prediction of El Nino-Southern Oscillation (Kondrashov et al., 2008).

In the present work, we have dealt with the problem of estimating physical parameters related with the sea-ice, using observations of sea-ice quantities. The issue is of great relevance given the large prediction error affecting coupled ocean-sea-ice model in Arctic area. The presence of new observations suppliers in recent years, including satellite-based instruments (see *e.g.* ICESat database), have motivated a stream of research aimed at their use to estimate sensitive sea-ice parameter. The present deliverable DL5.7 goes along this line of scope.

This reports describes the choice of method, the steps undergone and the results obtained at NERSC in the framework of SANGOMA. Taking advantage of the pre-existing Ensemble Kalman filter infrastructure at NERSC, the parameter estimation has been done using the EnKF in the augmented formulation. The standard sequential EnKF has been adopted at a first stage followed by the

Asynchronous EnKF later on, which allows for a compact way to assimilate observations distributed within a specified time window.

# Chapter 2

# Methodology

Two different EnKF strategies have been used in different stages of the work. First the sequential EnKF (Evensen, 2003) in its augmented formulation has been used to estimate three sea-ice parameters (Massonnet *et al.*, 2014). Then the asynchronous EnKF (Sakov *et al*, 2010) has been used for the same purposes, but the observations are now assimilated once at all at a single analysis time. The formulation of the parameter estimation problem also differs in the two stages. While global scalar quantities were estimated in the first case, the parameter spatial dependency was also quantified in the second case.

We have worked under a twin experiments setup, meaning that a run of the model is used to mimic the unknown true trajectory, in this case the parameters, we intend to estimate. Working with real observations will be the natural follow-on of the present exercise.

# Chapter 3

# Results

## 3.1 Case 1 - Sequential EnKF

The work has been done in collaboration with F. Massonnet at Université Catholique de Louvain la Neuve.

Here a method for calibration of parameters based on the ensemble Kalman filter is implemented, tested and validated in the ocean-sea ice model NEMO-LIM3. Three dynamic parameters are calibrated: the ice strength parameter $P^*$, the ocean-sea ice drag parameter $C_w$, and the atmosphere-sea ice drag parameter $C_a$. In twin, perfect-model experiments, the default parameter values are retrieved within 1 year of simulation. Using 2007-2012 real sea ice drift data, the calibration of the ice strength parameter $P^*$ and the oceanic drag parameter $C_w$ improves clearly the Arctic sea ice drift properties. It is found that the estimation of the atmospheric drag $C_a$ is not necessary if $P^*$ and $C_w$ are already estimated. The large reduction in the sea ice speed bias with calibrated parameters comes with a slight overestimation of the winter sea ice areal export through Fram Strait and a slight improvement in the sea ice thickness distribution. Overall, the estimation of parameters with the ensemble Kalman filter represents an encouraging alternative to manual tuning for ocean-sea ice models.

Complete results and the description of the approach are given in Massonnet *et al.*, 2014.

## 3.2 Case 2 - Asynchronous EnKF (AEnKF)

### 3.2.1 Model sensitivity to sea-ice parameters

Figure 3.1 shows the empirical distributions of $P^*$, $C_w$, and $C_a$ used to initialize the ensemble members. We have intentionally worked with a uniform distribution for $P^*$, and Gaussian for the two drag coefficients. This choice reflects our assumption on the uncertainty associated with the parameters. The red dots on the x-axis display the values used for each ensemble member. $N_{ens} = 30$ ensemble members are initialized in this first stage.

Figure 3.2 shows the ensemble mean and spread as a function of time, for three different experiments: (1), with only $P^*$ being perturbed, (2), with the two

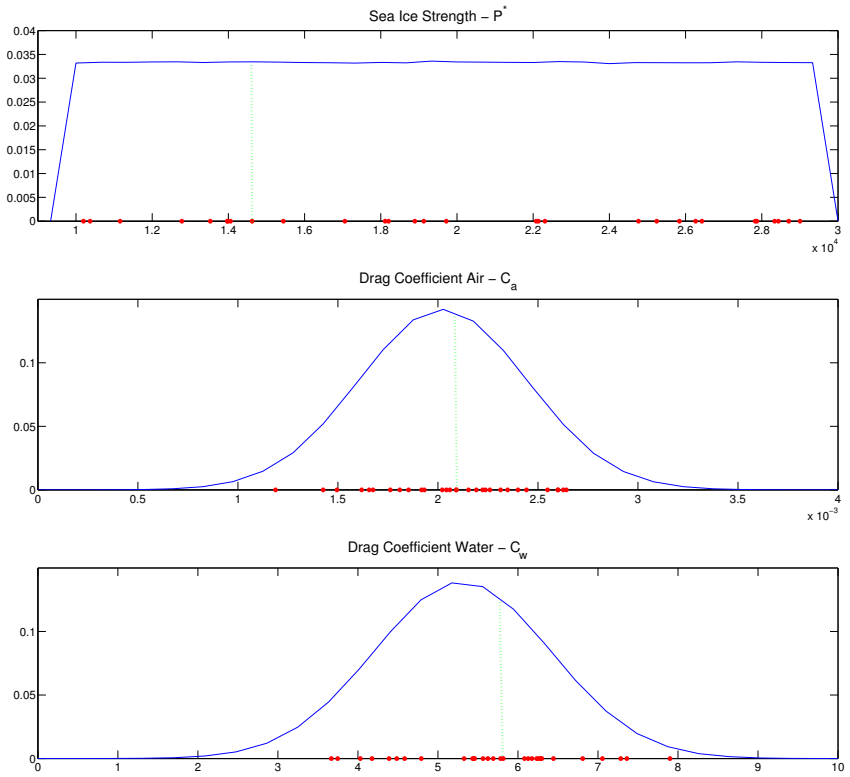


Figure 3.1: From top to bottom the empirical distributions used to sample $P^*$, $C_a$, and $C_w$ respectively. The red dots on the x-axis depict the values of the parameters used in the experiments, while the green vertical dot lines the value used in the twin experiments for reference.

drag coefficients simultaneously perturbed and (3) with the two $C$s and $P^*$ all perturbed. The figure illustrates the effect on the model sensitivity to the parameters under scrutiny. Results indicate that:

- The perturbations do not incur a significant bias in the ensemble mean (as one may have expected from the model nonlinearities).
- $P^*$ drives the ensemble spread in the sea-ice concentration ($Fice$) and thickness ($Hice$)
- The drag coefficients both act mainly on the sea-ice speed as expected.

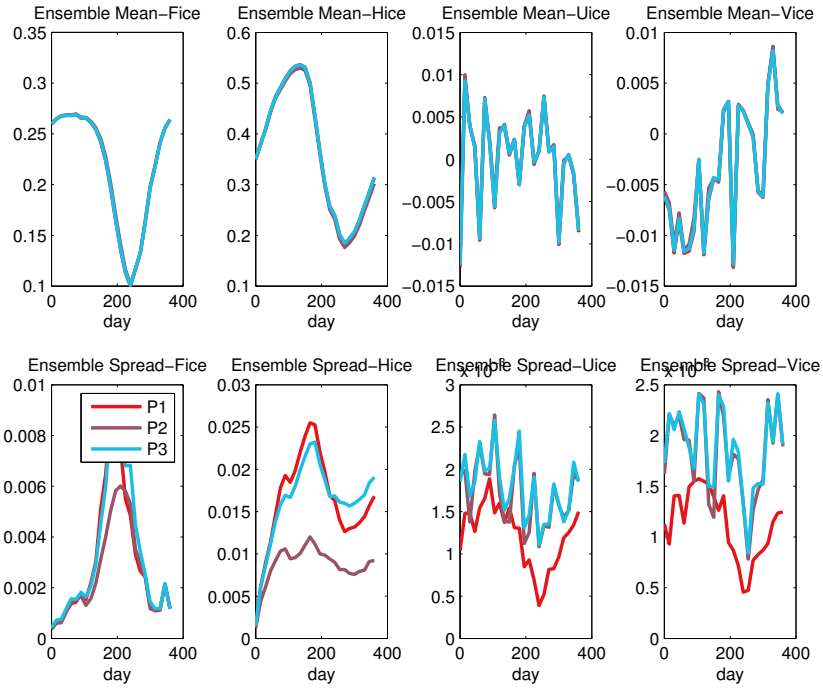


Figure 3.2: Ensemble Mean (top line) and Spread (bottom line) as a function of time for (from left to right) Fice, Hice, Uice and Vice. Days are counted from the 1st Jan.

In the P3 experiment, the effect is further highlighted in Fig. 3.3 to 3.6 that show the spatial patterns of the ensemble spread along 1-year of simulation at a display frequency of 3 months. The spread of ice concentrations is mostly confined to the ice edge (Fig. 3.3) while the spread of ice thickness gradually accumulates in the Beaufort Gyre (Fig. 3.4) and the spead of ice drift seems to have maximum amplitude along the main features of the circulation (Beaufort Gyre and Transpolar Drift, Figs. 3.5 and 3.6). These are the features that are expected from traditional manual tuning.

The sensitivity analysis reported in Figures 3.2 - 3.6 suggests that, when observing the sea-ice thickness, $P^*$ has the potential to be better estimated than the drag coefficients. Indeed, perturbing $P^*$ induces a larger spread in the sea-ice thickness, manifesting the correlation between the two quantities that is exploited

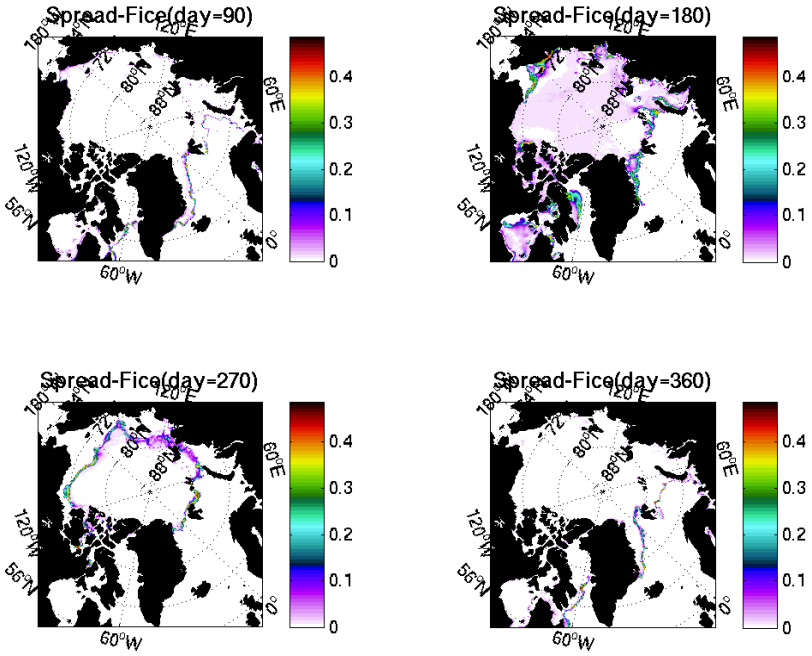


Figure 3.3: Ensemble Spread in the sea-ice concentration (Fice) at day (by row) 90, 180, 270 and 360. P3 experiment.

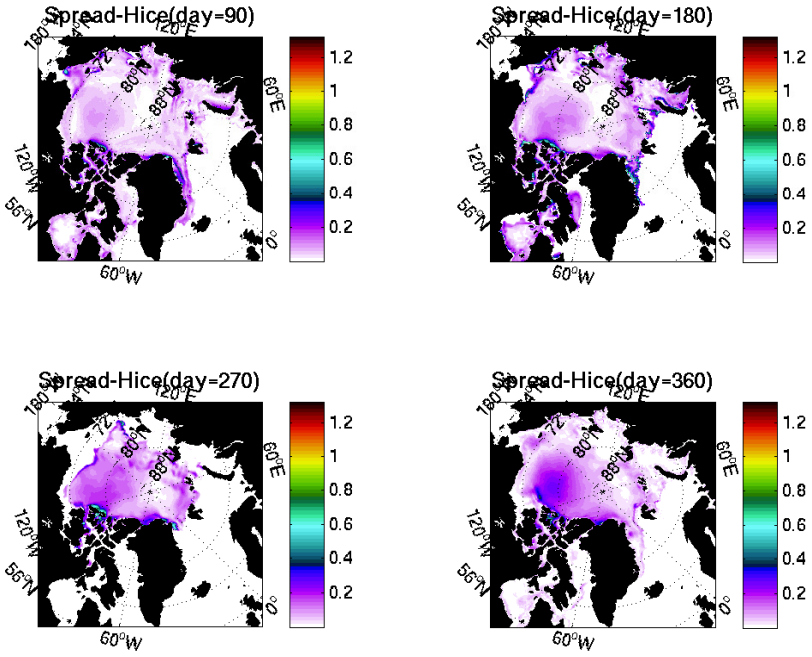


Figure 3.4: Same as Figure 3.3 but for sea-ice tickness (Hice).

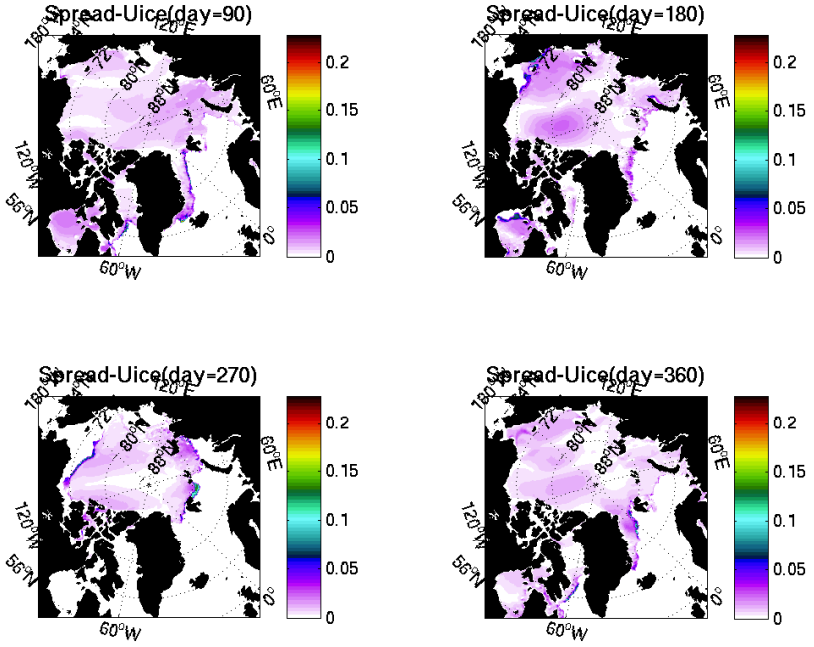


Figure 3.5: Same as Figure 3.3 but for sea-ice U-velocity (Uice).

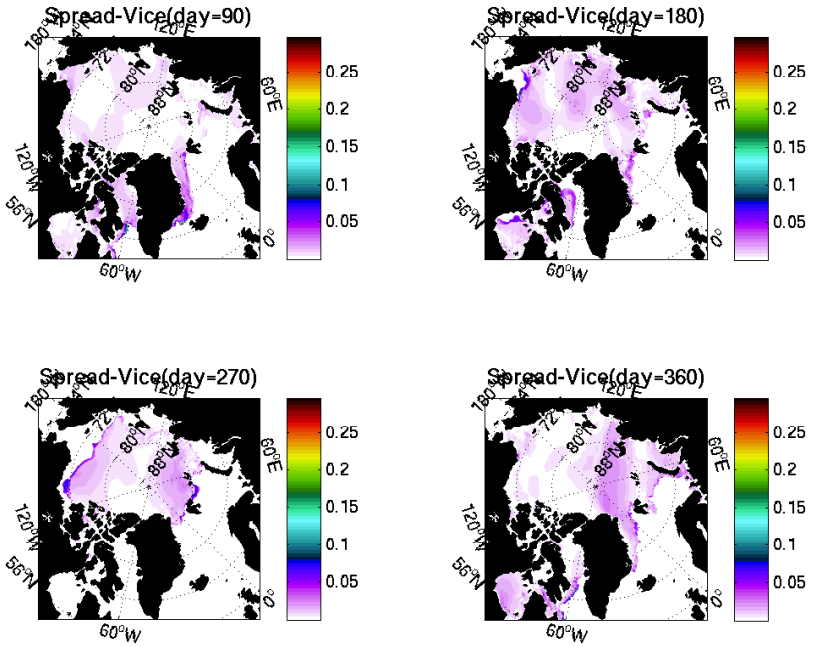


Figure 3.6: Same as Figure 3.3 but for sea-ice V-velocity (Vice).

Table 3.1: Forecast and Analysis Error in $P^*$

| | 1990 | 1991 | 1992 | 1993 | 1994 | 1995 |
|---|---|---|---|---|---|---|
| Forecast Error (N/m$^2$) | 5.9e+03 | 5.9e+03 | 5.9e+03 | 5.9e+03 | 5.9e+03 | 5.9e+03 |
| Analysis Error (N/m$^2$) | 5.4e+03 | 5.2e+03 | 5.0e+03 | 5.2e+03 | 5.4e+03 | 5.2e+03 |

at the analysis steps when observations of Hice are used to calibrate $P^*$. This conjecture is confirmed by the assimilation experiments that follow.

### 3.2.2 AEnKF with sea-ice thickness observations

As done in Section 3.1, we aim here at estimating dynamic parameters of the sea-ice, namely the sea-ice strength, $P^*$, and the two drag coefficients $C_w$, and $C_a$. Numerical experiments, under a perfect twin-experiment scenario have been carried out. The simulations span the period from 1989 to 1996, and parameter estimation is performed starting from 1990.

One key question of the SANGOMA WP5 is to evaluate the impact of new sea-ice observations. To this end, we focus here on the ability of sea-ice thickness observations to calibrate the aforementioned parameters. Synthetic observations of sea-ice thickness are simulated using by sampling one reference free model trajectory at the same geographical locations as the real ICESat observations. The latter are taken in two sampling campaigns per year in October-November and in February-March: in the experiments this situation is mimicked by taking the simulated observations at November and October the $1^{st}$ respectively. The simulated observational error variance for the hice thickness is set to $7.84 \times 10^{-2}$ (Zygmuntowska et *et al*, 2014). An ensemble of $24$ members is used, with an multiplicative inflation of $1\%$ and a localization via a Gaspari-Cohn modulating function with spatial scale equal to $800$ Km. The analysis is performed only once using the AEnKF, but observations are collected twice a year (at March and November) during the period from January 1990 to the analysis time.

Two types of experiments are considered: (1) estimation of the sea-ice strength, $P^*$, alone and, (2) estimation of the three parameters simultaneously. Figure 3.7 shows the analysis of $P^*$ at November 1990 and 1995. Each ensemble members is run using a different global value of $P^*$, but at the analysis times the spatial dependency of the parameter is also retrieved and is represented by the color shadows in the figure. The ability of the assimilation to reconstruct a geographical pattern for $P^*$ is apparent and the error is reduced in the largest areas of the domain: one of such an area is given in shadow grey in the left panel (North of the Canadian Archipelago and Greenland). The latter is computed as the difference between the spatial average of the analyzed $P^*$ and the reference value used as truth. Table 3.1 contains the forecast and analysis parametric error each year (November) in the period 1990 and 1995: it shows how the AEnKF leads to reducing the latter consistently. Nevertheless Fig. 3.7 also reveals that the assimilation returns nonphysical ($\leq 0$) values for $P^*$ (Laptev Sea, see the red shadow area in the right panel): this problem is currently under scrutiny. It may due to different implementation aspects of the assimilation such as the ensemble size, the inflation/localization setup, the number of observations among other.

The experiments of type (2), where the three parameters are simultaneously

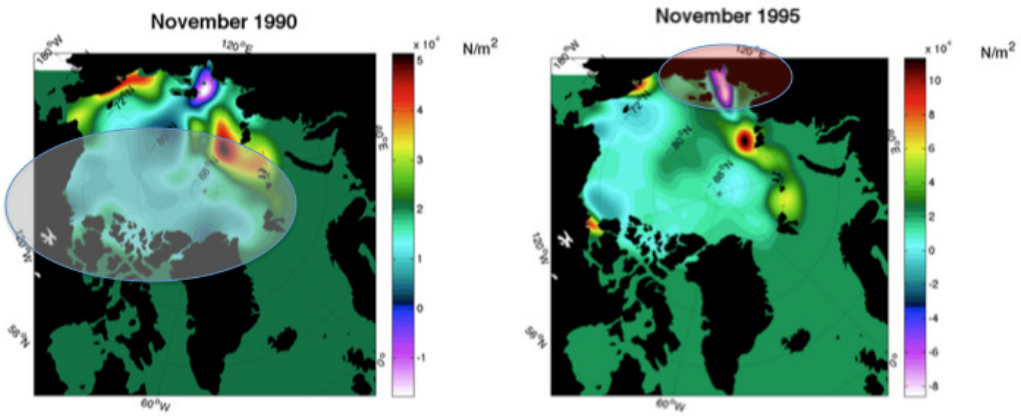


Figure 3.7: $P^*$ analysis field at November 1990 and 1995 using AEnKF

estimated have not given satisfactorily results. They indeed confirm what found in Massonnet et al., 2014, on the difficulty of calibrating the drags based on sea-ice thickness measurements as already anticipated when looking at the sensitivity analysis in the previous Section.

Fig. 3.8 shows the analysis field for $P^*$, $C_W$ and $C_a$ at November 1990 (top panels) and 1995 (bottom panels). As remarked in Fig. 3.7 the assimilation method and setup still require further optimization in view of the appearance of areas with nonphysical values ($\leq 0$). Moreover the field for the water drag coefficient, $C_W$, is also displaying a clear nonphysical discontinuity which is a further indication of imbalances created at the analysis step.

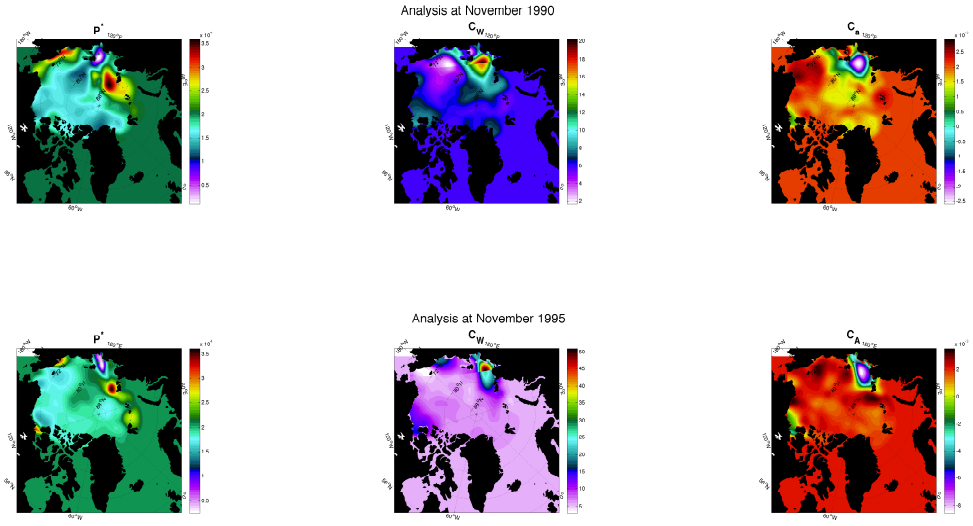


Figure 3.8: $P^*$, $C_W$ and $C_a$ analysis fields at November 1990 and 1995 using AEnKF

# Chapter 4

# Conclusion

SANGOMA WP5 has studied the use of sea-ice observations to calibrate dynamics sea-ice model parameters. The efforts were motivated by two combined factors, the known large errors of sea-ice models mainly originated by parameters mispecification and the rise of new observations (mainly from remote sensing) that offer a more homogeneous and consistent picture of the Arctic. The use of advanced data assimilation methods, at the core of SANGOMA's expertise, makes it possible to merge the model with observations and to address the question on how much observations can help reducing the parameter uncertainty.

The results depict a promising picture in that parameter error is indeed reduced is, as expected, the model has a marked sensitivity to the parameters intended to be estimated. This situation occurs, for instance, when using sea-ice thickness observations to calibrate the sea-ice strength. On the contrary, the same sea-ice thickness measurements are not useful to constraint error in the sea-ice strength and, overall the impact of data assimilation on the associated error seems only minor. Nevertheless further work is required in order to fix several implementation aspects of the data assimilation method. These issues are seen as the main causes behind the sporadic appearances of nonphysical values and discontinuity in the analysis fileds, and are the object of follow-on study.

More specifically, the ice thickness measurements are becoming more systematic with ESA's CryoSAT2 altimeter mission, which will be sustained with another ESA mission Sentinel-3. As CryoSAT2 and Sentinel-3 will observe ice thickness regularly and not only a few months per year, we expect that the parameter estimation will become more stable and will be taken up for the Copernicus Arctic MFC, which is based on the same AEnKF data assimilation system used in this report (i.e. the TOPAZ system).